ISSN 1063-7788, Physics of Atomic Nuclei, 2015, Vol. 78, No. 6, pp. 757–766. © Pleiades Publishing, Ltd., 2015.

NUCLEI
Experiment

Production of Isotopes and Isomers with Irradiation of $Z = 47–50$ Targets by 23-MeV Bremsstrahlung*

S. A. Karamian[1)**], J. J. Carroll[2)], N. V. Aksenov[1)], Yu. A. Albin[1)], A. G. Belov[1)], G. A. Bozhikov[1)], S. N. Dmitriev[1)], and G. Ya. Starodub[1)]

Received January 19, 2015; in final form, March 17, 2015

Abstract—The irradiations of Ag to Sn targets by bremsstrahlung generated with 23-MeV electron beams are performed at the MT-25 microtron. Gamma spectra of the induced activities have been measured and the yields of all detected radionuclides and isomers are carefully measured and analyzed. A regular dependence of yields versus changed reaction threshold is confirmed. Many isomers are detected and the suppression of the production probability is observed with growing product spin. Special peculiarities for the isomer-to-ground state ratios were deduced for the ^{106m}Ag, ^{108m}Ag, ^{113m}In, ^{115m}In, and ^{123m}Sn isomers. The production of such nuclides as ^{108m}Ag, ^{115m}In, ^{117g}In, and ^{113m}Cd is of interest for applications, especially when economic methods are available.

DOI: 10.1134/S1063778815060113

1. INTRODUCTION

Today, about 3500 nuclides are known including quite short-lived species. Evidently, halflives on the scale of milliseconds or shorter make them impractical for accumulation in amounts needed for the interdisciplinary research and applications. Yet there are many radionuclides that are valuable for the progress in the fields like medicine and technology. The production of those nuclides in the needed amounts is then a significant issue. Modern accelerators can effectively produce ion beams within a wide range of masses and with energies up to the order of TeV, so that intermediate- and high-energy accelerators are capable of producing many different nuclides in one irradiation. For example, tens to hundreds of different isotopes can result from proton spallation at 660 MeV [1] or from heavy-ion fragmentation [2].

Such wide coverage of the nuclide map from a single irradiation may be counterproductive when it is desired to produce one or a few specific nuclides in macroscopic amounts. Detection or separation of one definite isotope may be very difficult in the presence of backgrounds from other activities. High-precision techniques can indeed separate single ions for study [3], but these are not well-matched to production of large quantities of radionuclides. Moreover, each individual isotope will be produced with a relatively suppressed cross section when hundreds of nuclides arise simultaneously from the same irradiation. Overall, the accelerators to high energy may not be the best choice for production of radionuclides. In fact, the production of radionuclides by electron accelerators in the modest energy range of 15–30 MeV can be more practical. Such facilities are available at many laboratories and they are traditionally used in the mode of conversion of an electron beam to bremsstrahlung. Modern schemes provide [4] very high intensity of electron beams resulted in record brightness of the quasi-monochromatic photon source at 10–30 MeV. Such options are of particular value for accumulation of activities and for radiation physics. Photon-induced reactions at a moderate energy, less than about 30 MeV, offer the most efficient and economic way for production of radionuclides, since at higher photon energies many reaction channels open and it becomes necessary to apply separation techniques. Therefore, the emphasis in the present paper is on measurements for the production of radionuclides with the MT-25 electron accelerator to 23 MeV. In this range it is unnecessary to consider reactions leading to the multiple neutron emission or complex particles because they are suppressed compared to the major (γ, n) reaction.

Nuclear reactions induced by bremsstrahlung have been investigated for decades, but there is still more to be learned. For example, they were recently used [5–7] to clarify details of nuclear reactions, e.g. the manifestation of structural effects on the yields of reactions that are typically attributed to the statistical mechanism. Absorption of photons by the giant

*The text was submitted by the authors in English.

[1)]Joint Institute for Nuclear Research, Dubna, Russia.
[2)]US Army Research Laboratory, Maryland, US.
[**]E-mail: karamian@nrmail.jinr.ru

dipole resonance only slightly disturbs the single-particle orbitals in a nucleus; the electromagnetic wave impacts the nucleus as an object of definite size and shape since the wavelength for 15-MeV photons is comparable to the nuclear dimension, not to the size of the constituent particles. Thus, shell-model orbitals survive after photon absorption and their quantum numbers may influence the reaction yield with specific microstructure factors, in addition to the regular statistical ones. The statistical regularities visible in experimental yields are described [5] in a form of separate factors reflecting the reaction threshold and the spin difference between initial and final configurations. Nevertheless, some other structural effects in the reaction yields are newly found [6, 7] in reactions induced by photons and neutrons at low energies.

2. EXPERIMENT

For this work, activation experiments were performed using the MT-25 microtron of the Flerov Laboratory of Nuclear Reactions, Joint Institute for Nuclear Research. A 23 MeV electron beam of a power up to 0.3 kW was incident upon a tungsten "convertor" with 4 mm thickness. The residual energy of electrons was absorbed in the Al radiator with 25 mm thickness and the targets were placed for activation just behind this assembly at 0° to the beam. Light in weight targets ($\leqslant$0.5 g) have absorbed insignificant energy due to the exposure with bremsstrahlung without noticeable heat up of them. A stack of several different targets could be exposed simultaneously because of minor absorption of bremsstrahlung photons in the relatively thin target layers. Such an operation is useful for common calibration of the reaction yields resulted in the reduction of random scattering for measured values of relative yields. In one hour past irradiation, the samples were transported to HPGe detector for γ-ray activity measurements at clean room. The "cooling" for about one hour reduces the background counts due to the decay of short-lived products. For each sample, the spectra were measured at several times during an overall period of hours, days, or even months when long-lived products were looked for. The variations were undertaken in the sample-to-detector distance, cooling/counting times, and the use of γ-absorption filters between the sample and the detector. The aim was to provide optimal conditions for detection of all radioactive nuclides, even those appearing with low activity, when were produced due to the bremsstrahlung-induced reactions. Energy and efficiency calibrations of the detector were performed by spectra from γ-standard sources measured under identical conditions to those of the irradiated samples.

The spectrum of 23-MeV bremsstrahlung covers the giant dipole resonance (GDR) range for medium-mass nuclei. As is well known, the (γ, n) reaction is most probable in the energy range of the GDR and collects nearly all the photon absorption yield. The relative yields of other reactions, in ratio to the (γ, n) yield, provide experimental measurements of the probabilities for those individual reactions despite they are normally much less than 1. Likewise, the relative yields determine the probability for emission of protons or alphas [6], or for the population of high-spin isomers in the produced nuclei [5]. The isomer-to-ground state ratio is of interest in many cases. The activation technique, after careful yield calibration, provides reliable data for reaction-mechanism studies.

Targets of ^{109}Ag, ^{113}Cd, ^{114}Cd, $^{\mathrm{nat}}$Cd, $^{\mathrm{nat}}$In, and $^{\mathrm{nat}}$Sn were irradiated for periods of about 10 h. The gamma-ray spectra of the induced there activities were carefully measured. Figure 1 shows sections of two such spectra for ^{109}Ag and ^{114}Cd targets measured in 14 months past activation. The statistics of counts is enough to deduce the peak areas with moderately good accuracy. The long-lived ^{108m}Ag and ^{113m}Cd products are observed through the corresponding γ-ray lines. The spectra were processed using the commercial "Genie 2000" code to determine the energy and area of all distinguishable γ-ray peaks. The count rate for a peak attributed to a definite isotope corresponds to the number of nuclei of this species produced during the irradiation. The standard formulations were applied to account for the accumulation- and decay-time factors dependent on the irradiation, cooling, and measuring times. There were accounted: the quantum yield of the definite gamma ray, the detector efficiency, the filter transparency, etc. The spectroscopic data for all nuclides was obtained from compilations in "Nuclear Data Sheets."

The error of the relative yield of any product, compared to the (γ, n) yield, was obtained by standard error propagation. The accuracy of the deduced yield is determined as a combination of errors of different origin. The major ones are due to: the statistical error of the measured area for the γ line of interest, the usual inaccuracy in the detector efficiency calibration, and the systematic errors in the tabulated data.

In some cases, the self-absorption of gammas due to the sample thickness could not be neglected and corresponding corrections were inserted, with their own uncertainties. After all, an extremely high level of accuracy could not be reached in all cases. For the relative yield, standard deviations of about 8–25% were typical, as expected for the majority of measurements based on the γ-spectroscopic analysis. This

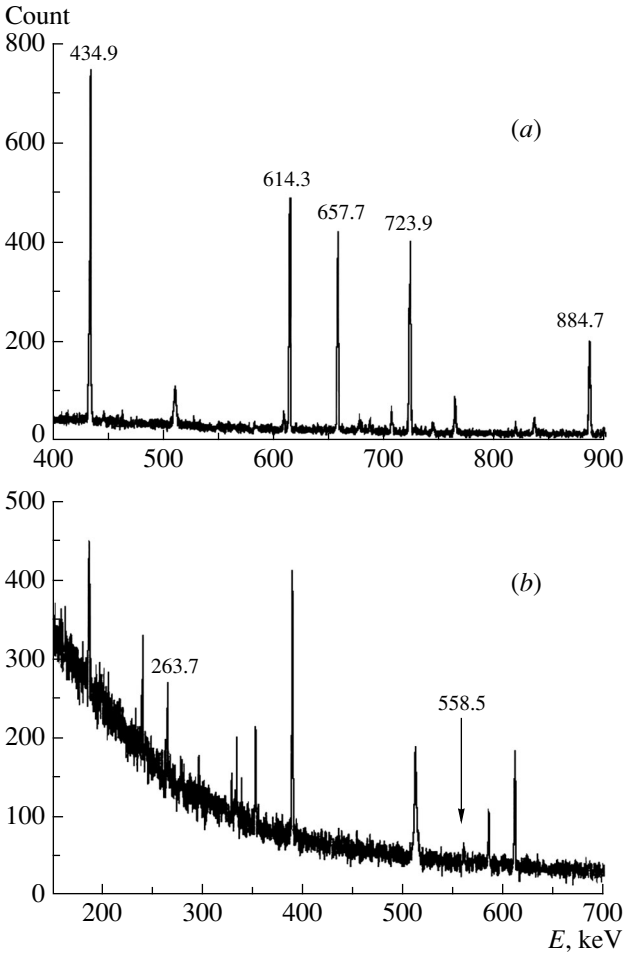

Fig. 1. Gamma-ray spectra measured in 14 months past irradiation of ^{109}Ag (a) and ^{114}Cd (b) targets. The lines of interest are indicated numerically: a—434.9, 614.3, 723.9 keV from ^{108m}Ag activity (past electron capture to ^{108}Pd) and 657.7, 884.7 keV from ^{110m}Ag activity (past β^- decay to ^{110}Cd); b—263.7-keV line corresponding to the ^{113m}Cd activity (past IT decay). Background lines are also visible, as well as a small peak at 558.5 keV due to prompt radiation emitted following the impurity ^{113}Cd(n, γ) reaction with the environment neutrons.

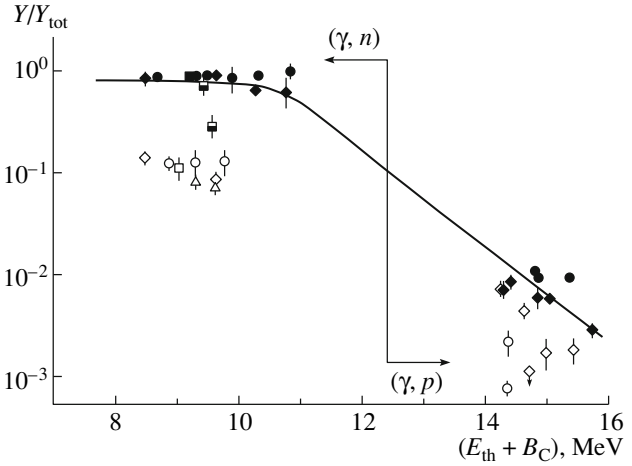

Fig. 2. Relative yield, Y/Y_{tot}, of (γ, n) and (γ, p) reaction products plotted vs. effective reaction threshold, $(E_{th} + B_C)$. The guide line corresponds to the total yield of the reaction. Target is specified by the symbol: triangles—Ag, circles—Cd, squares—In, diamonds—Sn. Filled symbols correspond to low spin-difference cases leading to ^{123m}Sn, ^{115g}Cd, ^{114g}In, ^{113g}Cd, ^{112g}In, ^{111g}Cd, ^{117g}Sn, ^{109g}Cd, ^{113g}Sn, ^{107g}Cd, ^{111}Sn, and ^{105}Cd from (γ, n) reactions, as well as ^{113m}In, ^{114g}In, ^{111g}Ag, ^{116g}In, ^{112g}Ag, ^{115m}In, ^{113g}Ag, and ^{117m}In from (γ, p) reactions; unfilled symbols indicate higher spin-difference cases leading to ^{123g}Sn, ^{115m}Cd, ^{114g}In, ^{113m}Cd, ^{108m}Ag, ^{112g}In, ^{106m}Ag, ^{117m}Sn, and ^{111m}Cd from (γ, n) reactions, as well as ^{113g}In, ^{110m}Ag, ^{114m}In, ^{115g}In, ^{116m}In, and ^{117g}In from (γ, p) reactions.

was nevertheless sufficient to obtain definite physical results. When the standard deviation exceeded 35%, only upper limit of the yield was obtained.

Reaction yields relative to the (γ, n) yield might be normalized to the number of target nuclei involved in the corresponding reaction. This procedure justified the use of multi-isotope targets, although some enriched targets were available, as well. In our case the (γ, n) reaction represents practically the total yield of photoabsorption, but, in general, the sum of all reaction products must be used and the measured data were sufficient for this analysis. Measured in the present experiment relative yields are given in Tables 1–5 for many reactions together with other parameters of importance, such as the effective reaction threshold, $(E_{th} + B_C)$. The threshold dependence of cross sections is one of the most general features in the phenomenology of nuclear reactions. For example, this is manifested by the Q_{gg}—systematic for transfer reactions with heavy ions [8, 9], for reactions with as light particles as ^{4}He [10], and recently for reactions with photons [5].

Relative yields measured in this work are shown in Fig. 2, plotted as a function of the effective reaction threshold, which includes the Coulomb barrier (B_C) for charged-particle emission. Its value was evaluated by the well-established formulation of [11] for the inverse process of the target–projectile fusion. The regular dependence seen in Fig. 2 confirms the causal correlation between the reaction probability and the threshold value for the group of reactions of different targets from Ag to Sn with 23-MeV bremsstrahlung. An anomalously low yield for (γ, α) reactions was clearly observed and has previously been explained in [6]. Here, the focus is on the most probable reactions: (γ, n) and (γ, p).

It was expected that the product yield in the reaction involving a high difference of spins between target and final nuclides would be suppressed due

Table 1. Reactions with ^{109}Ag enriched target

Reaction	Product	Spin values		Product halflife	E_γ, keV	Yield (error)	$(E_{th} + B_C)$, MeV
		target	product				
^{109}Ag (γ, n)	^{108m}Ag	1/2	6	438 yr	614 and 723	0.08(1)	9.30
^{109}Ag (γ, α)	^{105}Rh	1/2	7/2	35.4 h	319	$1.5(3) \times 10^{-4}$	13.56
^{107}Ag (γ, n)	^{106m}Ag	1/2	6	8.28 d	1045	0.07(1)*	9.63
^{107}Ag $(\gamma, 2n)$	^{105}Ag	1/2	1/2	41.3 d	345	$6.6(8) \times 10^{-2}$*	17.47

* Yields are reduced to the hypothetic ^{107}Ag target of 100% enrichment.

Table 2. Reactions with ^{113}Cd and ^{114}Cd enriched targets

Reaction	Product	Spin values		Product halflife	E_γ, keV	Yield (error)	$(E_{th} + B_C)$, MeV
		target	product				
^{113}Cd (γ, p)	^{112}Ag	1/2	2	3.12 h	617	$0.98(7) \times 10^{-2}$	14.89
^{113}Cd $(\gamma, 2n)$	^{111m}Cd	1/2	11/2	48.6 min	151 and 245	$1.5(9) \times 10^{-2}$	16.33
^{113}Cd (γ, α)	^{109}Pd	1/2	5/2	13.7 h	88	$2.4(6) \times 10^{-4}$	14.32
^{114}Cd (γ, n)	^{113m}Cd	0	11/2	14.1 yr	264	0.12(1)	9.31
^{114}Cd (γ, p)	^{113}Ag	0	1/2	5.37 h	299	$0.94(7) \times 10^{-2}$	15.40
^{114}Cd (γ, d)	^{112}Ag	0	2	3.12 h	617	$1.4(4) \times 10^{-4}$	20.98

Table 3. Reactions with ^{nat}Cd target

Reaction	Product	Spin values		Product halflife	E_γ, keV	Yield (error)	$(E_{th} + B_C)$, MeV
		target	product				
^{116}Cd (γ, n)	^{115g}Cd	0	1/2	53.46 h	528	0.88(3)	8.70
	^{115m}Cd	0	11/2	46.61 d	934	0.123(12)	8.88
^{114}Cd (γ, n)	^{113m}Cd	0	11/2	14.1 yr	264	0.125(18)	9.31
^{114}Cd (γ, p)	^{113}Ag	0	1/2	5.37 h	299	$0.89(6) \times 10^{-2}$	15.40
^{113}Cd (γ, p)	^{112}Ag	1/2	2	3.13 h	617	$0.90(6) \times 10^{-2}$	14.89
^{112}Cd (γ, n)	^{111m}Cd	0	11/2	48.6 min	151 and 245	0.128(25)	9.79
^{112}Cd (γ, p)	^{111}Ag	0	1/2	7.45 d	342	$1.05(5) \times 10^{-2}$	14.83
^{111}Cd (γ, p)	^{110m}Ag	1/2	6	249.9 d	658	$0.71(9) \times 10^{-3}$	14.37
^{110}Cd (γ, n)	^{109}Cd	0	5/2	462 d	88	0.86(10)	9.92
^{108}Cd (γ, n)	^{107}Cd	0	5/2	6.50 h	93.5	0.907(30)	10.35
^{108}Cd (γ, d)	^{106m}Ag	0	6	8.28 d	1045	$1.1(3) \times 10^{-4}$	20.07
^{106}Cd (γ, n)	^{105}Cd $\rightarrow$ ^{105}Ag	0	5/2 $\rightarrow$ 1/2	56 min $\rightarrow$ 41.3 d	345	1.00(12)	10.87
^{106}Cd $(\gamma, 2n)$	^{104}Cd $\rightarrow$ ^{104m}Ag	0	0 $\rightarrow$ 2	58 min $\rightarrow$ 33.5 min	556	$0.6(2) \times 10^{-2}$	19.30

Table 4. Reactions with ^{nat}In target

Reaction	Product	Spin values		Product halflife	E_γ, keV	Yield (error)	$(E_{th} + B_C)$, MeV
		target	product				
$^{115}\mathrm{In}\,(\gamma,\gamma')$	$^{115m}\mathrm{In}$	9/2	1/2	4.49 h	336	$2.34(14)\times10^{-2}$	0.336
$^{115}\mathrm{In}\,(\gamma,n)$	$^{114m}\mathrm{In}$	9/2	5	49.51 h	190	0.89(2)	9.23
$^{115}\mathrm{In}\,(\gamma,2n)$	$^{113m}\mathrm{In}$	9/2	1/2	1.66 h	392	$1.0(3)\times10^{-2}$	16.70
$^{115}\mathrm{In}\,(\gamma,\alpha)$	$^{111}\mathrm{Ag}$	9/2	1/2	7.45 d	342	$4.5(8)\times10^{-5}$	14.45
$^{113}\mathrm{In}\,(\gamma,n)$	$^{112g}\mathrm{In}$	9/2	1	15.0 min	617 and 606	0.72(9)	9.45
	$^{112m}\mathrm{In}$	9/2	4	20.6 min	156	0.28(6)	9.61
$^{113}\mathrm{In}\,(\gamma,2n)$	$^{111}\mathrm{In}$	9/2	9/2	2.81 d	245 and 171	0.063(17)	17.11
$^{113}\mathrm{In}\,(\gamma,d)$	$^{111m}\mathrm{Cd}$	9/2	11/2	48.6 min	151	$\approx 0.9\times10^{-3}$	18.42

Table 5. Reactions with ^{nat}Sn target

Reaction	Product	Spin values		Product halflife	E_γ, keV	Yield (error)	$(E_{th} + B_C)$, MeV
		target	product				
$^{124}\mathrm{Sn}\,(\gamma,n)$	$^{123g}\mathrm{Sn}$	0	11/2	129.2 d	1088	0.14(6)	8.49
	$^{123m}\mathrm{Sn}$	0	3/2	40.1 min	160	0.86(9)	8.51
$^{119}\mathrm{Sn}(\gamma,\alpha)$	$^{115}\mathrm{Cd}$	1/2	1/2	53.46 h	528	$3.9(8)\times10^{-5}$	15.31
$^{118}\mathrm{Sn}\,(\gamma,n)$	$^{117m}\mathrm{Sn}$	0	11/2	13.6 d	159	$8.5(1.0)\times10^{-2}$	9.64
$^{118}\mathrm{Sn}\,(\gamma,p)$	$^{117}\mathrm{In}$	0	9/2	43.2 min	553	$1.7(3)\times10^{-3}$	15.45
	$^{117m}\mathrm{In}$	0	1/2	1.94 h	315	$2.7(4)\times10^{-3}$	15.76
$^{117}\mathrm{Sn}\,(\gamma,p)$	$^{116m}\mathrm{In}$	1/2	5	54.3 min	1097	$1.6(5)\times10^{-3}$	15.01
$^{116}\mathrm{Sn}\,(\gamma,p)$	$^{115m}\mathrm{In}$	0	1/2	4.49 h	336	$5.6(4)\times10^{-3}$	15.07
$^{115}\mathrm{Sn}\,(\gamma,p)$	$^{114m}\mathrm{In}$	1/2	5	49.51 h	190	$4.2(6)\times10^{-3}$	14.39
$^{114}\mathrm{Sn}\,(\gamma,n)$	$^{113}\mathrm{Sn}$	0	1/2	115.1 d	392	0.65(5)	10.30
$^{114}\mathrm{Sn}\,(\gamma,p)$	$^{113m}\mathrm{In}$	0	1/2	1.66 h	392	$6.8(9)\times10^{-3}$	14.32
$^{112}\mathrm{Sn}\,(\gamma,n)$	$^{111}\mathrm{Sn}\rightarrow{}^{111}\mathrm{In}$	0	$7/2\rightarrow9/2$	35 min $\rightarrow$ 2.91 d	245	0.62(22)	10.79
$^{112}\mathrm{Sn}\,(\gamma,2n)$	$^{110}\mathrm{Sn}\rightarrow{}^{110m}\mathrm{In}$	0	$0\rightarrow2$	4.15 h $\rightarrow$ 1.15 h	658	$5.4(1.6)\times10^{-3}$	18.96

to a "spin factor" [5] that reflects the reduced level density [12] for higher-spin states of the final nucleus compared to the initial one. Recall that in the statistical approach for the system of many particles, the probability of a process is defined by the number of micro-states available at definite excitation of the ensemble. As is evident in Fig. 2, the relative yields for reactions corresponding to high difference between the product and the target spins are located below the yield of reactions with low spin differences. The high-spin difference is typical for isomer production. Both isomeric and ground state yields are independently presented in Fig. 2, again relative to the total yield of the definite reaction. In some cases, only the isomer or ground-state yield could be measured in the experiment due to a short or very long halflife for the other state. Then the complementary (unmeasured) product yield was determined with a "missing yield" method, by taking the difference between the total reaction yield and the measured one. Total yield follows the curve shown in Fig. 2 as function of the $(E_{th} + B_C)$ parameter.

It is also possible to find some isomers that are characterized by low spin, while the ground state

Table 6. Measured and deduced yields of the m and g states taken as a ratio to the total yield of the concrete reaction Y_r

Target	Spin	Reaction	Product	Spin	ΔI	Y/Y_r
^{109}Ag	1/2	(γ, n)	^{108m}Ag	6	11/2	0.08
^{107}Ag	1/2	(γ, n)	^{106m}Ag	6	11/2	0.07
^{116}Cd	0	(γ, n)	^{115g}Cd	1/2	1/2	0.88
			^{115m}Cd	11/2	11/2	0.12
^{114}Cd	0	(γ, n)	^{113m}Cd	11/2	11/2	0.105
^{112}Cd	0	(γ, n)	^{111m}Cd	11/2	11/2	0.128
^{111}Cd	1/2	(γ, p)	^{110m}Ag	6	11/2	0.075
^{108}Cd	0	(γ, d)	^{106m}Ag	6	6	0.05
^{115}In	9/2	(γ, n)	^{114g}In	1	−7/2	0.09
			^{114m}In	5	1/2	0.91
		$(\gamma, 2n)$	^{113g}In	9/2	0	0.84
			^{113m}In	1/2	−4	0.16
^{113}In	9/2	(γ, n)	^{112g}In	1	−7/2	0.72
			^{112m}In	4	−1/2	0.28
		(γ, d)	^{111g}Cd	1/2	−4	≈0.3
			^{111m}Cd	11/2	1	≈0.7
^{124}Sn	0	(γ, n)	^{123g}Sn	11/2	11/2	0.14
			^{123m}Sn	3/2	3/2	0.86
^{118}Sn	0	(γ, n)	^{117m}Sn	11/2	11/2	0.085
		(γ, p)	^{117g}In	9/2	9/2	0.39
			^{117m}In	1/2	1/2	0.61
^{117}Sn	1/2	(γ, p)	^{116m}In	5	9/2	0.22
^{116}Sn	0	(γ, p)	^{115m}In	1/2	1/2	0.76
^{115}Sn	1/2	(γ, p)	^{114m}In	5	9/2	0.54
^{114}Sn	0	(γ, p)	^{113m}In	1/2	1/2	0.90

has a high spin, in contrast to the typical situation. Therefore, it can be expected that low-spin isomers are populated with high probability from low-spin targets. The isomer-to-ground state ratio is correspondingly inverted comparing to standard higher spin for the isomer. That is confirmed in experiments. The odd-mass indium nuclides are obvious examples of such an anomaly and their isomer-to-ground-state ratios are discussed in more detail below. In Fig. 2, the points are split onto two groups characterized by low and high *spin difference* of the product and target nuclei and not simply by the product spin, as is assumed in some papers. The preferential population of states corresponding to low spin difference is evident.

It is well known that branching of radioactive decay is also regulated by the spin difference between initial and final states. For example, a high-spin isomer populates more easily the high-spin levels of the decay product if available. The preferential decay sequences for Cd nuclides are shown in Fig. 3, where selectivity due to spin differences between mother and daughter nuclei is evident. Whether created in reactions induced by bremsstrahlung, by neutrons, or by fission, those Cd nuclides serve as predecessors for the generation of activities of: ^{115m}In, ^{117g}In, ^{117m}In, ^{119m}In, and of ^{117m}Sn, ^{119m}Sn past second decay. The latter products are of interest for nuclear medicine. Their direct production by (n, γ) and (γ, n)

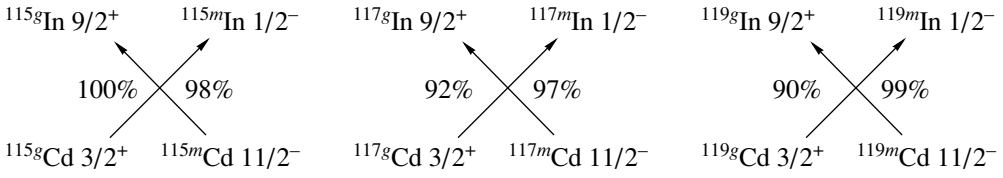

Fig. 3. Decay consequence for β^- radioactive Cd nuclides.

reactions is fail because of identical element in the target/product couple. That makes impossible the chemical isolation of the activity of interest from the ballast material and reduces the specific activity to a low value. However, the accumulation past decay of a mother activity allows for chemical isolation of the daughter species of interest. This variant got the name of the "generator" method when high specific-activity ^{99m}Tc sources were supplied for medicine practice. We indicate now that "generator" also could operate well for the radioactive species of indium.

It is now stressed that population of reaction products clearly demonstrates a similar spin selectivity as seen in radioactive-decay chains (Fig. 3), despite reaction mechanisms being very different from the beta decay. Nevertheless, a correlation between initial- and final-state spins takes place. For instance, the low-spin isomers ^{113m}In, ^{115m}In, and ^{123m}Sn are populated with a greater probability in bremsstrahlung-induced reactions with low-spin targets, as is clear from Table 5. Interestingly, even at much higher electron energies of 50–70 MeV, the lower-spin species are preferentially populated, whether they are isomers or ground states [13]. The present data confirms that photonuclear reactions are driven by the threshold and spin factors in accordance to the conclusion of analysis [5] based on the earlier published results. This approach does not contradict first principles of physics and in concrete manifestation creates a platform for comparison of the reactions and supplies the basis for predictions.

3. SPECIAL PECULIARITIES IN THE REACTION–YIELD BEHAVIOR

Figure 2 serves for illustration of the physical yield (probability) dependence on threshold and spin factors. Some special manifestations could be distinguished after analysis in more detail.

3.1. Yields of Reactions with In Target

The measured and deduced yield values are given in Table 6 separately for m and g states, thus, the m/g ratio could be deduced immediately. Unlike Tables 1–5, the calibration of yields is arranged to the yield of concrete reaction, not necessarily to the total yield. When one of two m and g states is only measured, the reaction yield is not defined directly but it could be assumed the same as for similar reaction with the neighbor-target nuclide. This is the case of "deduced" yield. The values of product–target spin difference in reaction, $\Delta I = I_p - I_t$, are given in Table 6 and lower m/g ratios are evident for greater ΔI step in reaction. The anomaly for ^{113}In, ^{115}In targets is known because high-spin 9/2 corresponds to the ground state and 1/2 to the isomers. Such an abnormal order takes no place for even-mass In isotopes. Some reactions with ^{113}In and ^{115}In are characterized with negative ΔI, but it is not necessarily accomplished with a high m/g ratio. Similar anomaly is also known for the ^{89m}Zr, ^{92m}Nb, and ^{91m}Mo isomers and the yield of the low-spin isomers was interpreted in [14] attracting the shell-model structure of nuclides near the closed neutron shell $N = 50$. Let's compare to $Z = 49$ for In.

The reactions with stable ^{113}In and ^{115}In nuclides lead to the initial population of high-spin states and past neutron emission, to the high-spin isomer, or to low-spin ground state. In the latter case, the regular spin decrease in γ cascade is required because ΔI is negative in an absolute value. Normally, when ΔI is positive, the spin deficiency takes place and the angular momentum enough for isomer population must be accumulated in the statistical γ cascade. However, a probability of the regular build-up of spin in statistical γ cascade is not high. Therefore, the m/g ratio is typically a much lower unity. Now we formulate the problem: whether this is also true for the case of negative ΔI. Reduction of the spin may happen through the stretched cascade of transitions within the collective band. A high m/g ratio could be eventually reached. But in reality, as is visible in Table 6, the m/g ratio is not always high at negative ΔI.

The results listed in Table 6 are also reduced in Fig. 4. They are presented versus ΔI (Fig. 4*a*), and in Fig. 4*b*—versus a new spin-difference parameter introduced in [5] basing on the following arguments. The reaction yield in statistical approach correlates with the level density of the excited product which is dependent on the spin square. Points in Fig. 4, as normally, are scattered due to the random inaccuracy

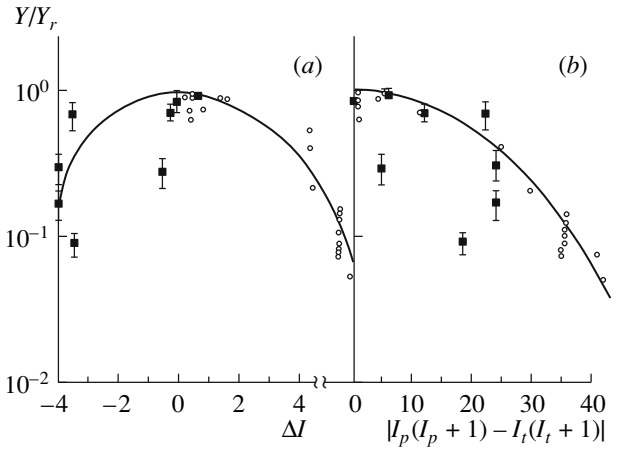

Fig. 4. Partial yields of m and g states as a ratio to the specific reaction yield Y_r plotted vs. $\Delta I(a)$, or vs. a new spin-difference parameter (b). Black squares—reactions with ^{113}In and ^{115}In targets; open circles—other reactions. The guide line is drawn through the open circles.

of the experimental data and due to the manifestation of nuclear-level scheme's peculiarities. The latter effect looks also random when the points for different reactions are displayed all together. It is evident that the scattering of points is reduced in Fig. 4*b*, compared to Fig. 4*a*, because the new parameter of the spin-square difference ($|I_p(I_p+1) - I_t(I_t+1)|$) taken in an absolute value is better relevant to the described process. The reaction yield correlates with the level density of the excited product and the level density is dependent on the spin square [12]. Naturally, the choice [5] for a new parameter of spin difference is now confirmed by the additional set of data, in particular, corresponding to the high-spin targets.

Black points in Fig. 4*b* (In) deviate not as much from other points, i.e. the yield is decreased versus the absolute value of the spin-square difference, independently on the sign of ΔI. Such symmetry shows that direct population of the high-spin members of collective bands (needed for the cascade with the regular spin decrease) is not very probable in the studied reactions. Obviously, the GDR-doorway mode excited past photon absorption is physically decoupled from the collective-band modes. The population of final states, in general, follows the statistical trend and the statistical spin factor remains significant because of the angular momentum conservation. This does not cancel the structure mixing at moderate and high excitation energies. The irregularities are yet possible, for instance, as is seen for two black points in Fig. 4*b*.

Taking into account the previously known and these new results, one concludes that a high initial spin promotes population of the high-spin product and the low spin leads to the similar one. But, the *transition from low to high spin is suppressed and, surprisingly, the same is valid from high to low spin ones*. This observation, being correct in many cases, does not reach as strong status as the quantum-number conservation. Statistical trends involve the "random" deviations connected with the individuality of a concrete nucleus.

3.2. Production of the ^{115m}In and ^{117g}In Therapeutic Radionuclides

The 13.6 d lived ^{117m}Sn isomer looks perspective [15] for medical application because of a moderate lifetime and attractive properties of the decay radiation, mostly of the conversion electrons. It could be produced through the ^{116}Cd (^{4}He, $3n$) reaction with a good cross section and m/g ratio. But expenses for the cyclotron beam restrict this method in practical application. The irradiations by low-energy bremsstrahlung are more economic and productive, especially in a view of high-intensity electron beams available over the world, see, for example, in [4]. The yield of this isomer in ^{118}Sn (γ, n) reaction is now reliably measured and the m/g ratio $\approx$0.09 seems acceptable. The activity at the scale of about 0.05 Ci in equilibrium could be reached with the electron beam of moderate power (1 kW). However, radionuclide is accumulated within the tin-target material restricting the chemical isolation procedure and reducing the specific activity.

There is known the experimental scheme of the "generator" method applied successfully for the accumulation of ^{99m}Tc ($T_{1/2} = 6$ h) from the source of ^{99}Mo ($T_{1/2} = 66$ h). The latter nuclide could be stored in a great amount at previous irradiations through the (n, γ), (γ, n), or $(n, 2n)$ reactions [15]. Technetium is successfully separated from Mo with chemical methods. It looks attractive to propose a similar generator scheme for ^{117m}Sn: ^{116}Cd(n, γ) ^{117m}Cd, 3.36 h $\rightarrow^{117g}$In, 43.2 min $\rightarrow^{117m}$Sn, 13.6 d. The spin values for the product nuclides are changed over this chain as: $11/2 \rightarrow 9/2 \rightarrow 11/2$, i.e. it seems favorable for the good branching ratios. However, due to random reasons, the final decay branch turns out [16] to be as low as of about 0.4%. Thus, the generator scheme is inefficient for ^{117m}Sn, but this chain works well till the ^{117}In products: ^{116}Cd $(n, \gamma)^{117g/m}$Cd, 2.49/3.36 h $\rightarrow^{117m/g}$In, 1.94/0.72 h. Even more attractive looks the generator scheme for accumulation of the ^{115m}In isomer: ^{116}Cd$(\gamma, n)^{115g}$Cd, 53.4 h $\rightarrow^{115m}$In, 4.49 h. The same as ^{99m}Tc, ^{115m}In is accumulated in decay of the longer-lived predecessor and the ratio for the mother to daughter $T_{1/2}$ appears

similar in both cases. Finally, ^{115m}In and ^{117m,g}In nuclides could be produced in the generator scheme allowing for the chemical isolation of In from the ballast Cd target-material. The decay branches are very advantageous in these cases (see Fig. 3), while In radionuclides are of interest for therapy of patients.

3.3. Production of the Long-Lived ^{108m}Ag and ^{113m}Cd Isomers

Fifteen years ago, there was formulated a possibility to use the long-lived isomers for storage of the nuclear energy with consequent release of it by demand, see [17] and references therein. The ^{178m2}Hf isomer was selected as the best because of high excitation energy of 2.45 MeV a nucleus and long halflife of 31 years. However, extensive experimental studies [18] do not support the possibility of artificial release of the isomeric energy induced by external irradiation. Then others, more promising isomers, were looked for the successful triggering. After analysis of nuclear spectroscopy data, it was deduced [19] that the triggering path for some isomers may be arranged through the excitation of the definite level located a little above the isomeric state. The most promising schemes are found for the following nuclides: ^{108m}Ag, ^{113m}Cd, ^{125m}Te, and ^{166m}Ho because the appropriate "gateway" levels were really observed, according to the known data. Additional spectroscopic studies were then arranged for ^{108}Ag in [20] and the direct attempt to observe the ^{108m}Ag triggering was undertaken in [21].

In the present work, the yields of ^{108m}Ag and ^{113m}Cd isomers in (γ, n) reactions are successfully detected, despite very long halflife (438 yr) of ^{108m}Ag and low γ-line yield (2.7×10^{-4}) per decay of 14.1 years-lived ^{113m}Cd. In the experiment, the count rate for γ lines of these isomers was low, but detectable. The productivity looks reasonably high when it is expressed in a number of atoms, and not in SI. After analysis, one deduces that about $(1-1.5) \times 10^{15}$ atoms must be reached due to the one-month irradiation of 5-g of enriched ^{109}Ag, or ^{114}Cd targets by the bremsstrahlung generated with 1-kW electron beam. Naturally, this yield must be linearly enlarged with the increased irradiation time, or/and the beam power. The electron beams of MW power are achievable at modern accelerators. The production via (γ, n)-reaction method is efficient for accumulation of ^{108m}Ag and ^{113m}Cd isomers in an amount of milligrams for future experiments on their triggering.

The yields of ^{106g}Ag and ^{108g}Ag states remain unmeasured in the present experiment because of relatively short lifetimes. Strictly speaking, they could be detected, but with a great uncertainty—since $T_{1/2}$ is much shorter than the irradiation time. The total yield calibration was performed using the results on activation of the Cd target at the same conditions. The integral GDR cross sections for Ag and Cd are almost identical, as follows from the well-known "Atlas of photonuclear data" [22]. Due to this calibration, the isomer-to-ground-state ratios are found to be 0.08 for ^{108m}Ag and 0.12 for ^{113m}Cd. The production of ^{108m}Ag in (n, γ) reaction is ready for comparison. The reliable data is available since this reaction was used for preparation of the ^{108m}Ag sources. The ratio $m/g \approx 0.06$ was observed for the (n, γ) reaction according to [23]. This is a little lower compared to the present results taken with the (γ, n) reaction. Such a deviation serves rather to confirm the correctness of both figures for m/g ratios in (γ, n) and (n, γ) reactions, than to establish the contradiction. As known, the probability of high-spin isomer population is typically lower in (n, γ) than in (γ, n) reactions.

The m/g ratios now obtained for other (γ, n) reactions are easily deduced from the data given in the tables. The higher-to-lower spin ratios for ^{111m}Cd, ^{113m}Cd, ^{115m}Cd, ^{117m}Sn, and ^{123g}Sn nuclides remain within the range from 0.10 to 0.14. All listed nuclei possess the spin quantum number equaling 11/2, almost the same as 6 for ^{106m}Ag and ^{108m}Ag. For the latter isomers, the m/g ratio is significantly lower, by 30–50% which could be explained by a specific scheme of low-excited levels. It was established in [20] that the isomeric 6^+ state in ^{108}Ag is strongly linked to the dipole bands of negative parity. There are twin-bands expanded up to high spin and excitation energy. Probably, these bands are not strongly populated in the (γ, n) reactions because the GDR doorway mode excited past photon absorption is physically decoupled from the rotation/vibration modes. The similarity is evident to the discussed above case of the final-state population in reactions with the In target. Such peculiarities may confirm the microstructure manifestation in the yield of products even for the reactions generally treated within the statistical mechanism. The microstructure role in reactions was also discussed in [7].

4. SUMMARY

Applying the activation method, relative yields (probabilities) of different reactions were measured for interactions of 23-MeV bremsstrahlung with Ag to Sn targets. The radioactive products were detected by γ-spectroscopy techniques. There was found a common for all targets regular dependence of yields from the threshold and spin factors. Such a factorization was proposed in our earlier publication [5] and now

is confirmed by additional experimental data. After analysis, some peculiarities were established: (a) special behavior of the m/g ratios in reactions with ^{113}In and ^{115}In targets due to the inversion of the spin order for the ground and isomeric states; (b) reduced m/g ratio for ^{106m}Ag and ^{108m}Ag which could be explained by the influence of specific level scheme onto the reaction yield. The innovative variant of a "generator" scheme is proposed for production in (γ, n) reaction of pure ^{115m}In and ^{117m,g}In radioactive species useful for the therapy of patients. The productivity of the (γ, n) reaction was measured also for accumulation of the long-lived ^{108m}Ag and ^{113m}Cd isomers. Level schemes of these nuclei are promising for the nuclear energy release by demand since the photons with energy as low as 260 keV could be efficient for the stimulation of isomer depletion.

ACKNOWLEDGMENTS

The reported study was partially supported by RFBR, research project no. 14-03-00745a.

REFERENCES

1. S. A. Karamian, J. Adam, D. V. Filossofov, et al., Nucl. Instrum. Methods Phys. Res. A **489**, 448 (2002).
2. A. Heinz, K.-H. Schmidt, A. R. Junghans, et al., Nucl. Phys. A **713**, 3 (2003).
3. L. Chen, P. M. Walker, H. Geissel, et al., Phys. Rev. Lett. **110**, 122502 (2013).
4. C. Borcea, in *Proceedings of the International Symposium on Exotic Nuclei* (World Scientific, Singapore, 2013), p. 401.
5. S. A. Karamian, Phys. At. Nucl. **76**, 1437 (2013).
6. S. A. Karamian, Phys. At. Nucl. **77**, 1429 (2014).
7. S. A. Karamian, in *Proceedings of the QFTHEP Workshop, Repino, St.-Petersburg, 2013. http://pos.sissa.it*
8. V. V. Volkov, Phys. Rep. **44**, 93 (1978).
9. A. Winther, Nucl. Phys. A **594**, 203 (1995).
10. S. A. Karamian, J. J. Carroll, N. V. Aksenov, et al., Nucl. Instrum. Methods Phys. Res. A **646**, 87 (2011).
11. R. Bass, Nucl. Phys. A **231**, 45 (1974).
12. A. Gilbert and A. G. W. Cameron, Can. J. Phys. **43**, 1446 (1965).
13. Md. Shakilur Rahman, Kyung-Sook Kim, Manwoo Lee, et al., Nucl. Instrum. Methods Phys. Res. B **268**, 13 (2010).
14. V. M. Mazur, Z. M. Bigan, and I. V. Sokolyuk, Laser Phys. **5**, 273 (1995).
15. S. C. Srivastava and L. F. Mausner, Med. Radiol. **174**, 782 (2012).
16. J. Blachot, Nucl. Data Sheets **95**, 679 (2002).
17. P. M. Walker and J. J. Carroll, Nucl. Phys. News **17** (2), 11 (2007).
18. J. J. Carroll, S. A. Karamian, R. Propri, et al., Phys. Lett. B **679**, 203 (2009).
19. S. A. Karamian and J. J. Carroll, in *Proceedings of the International Conference on Isomers in Nuclear and Interdisciplinary Research, Peterhof, St.-Petersburg, 2011*, JINR Preprint No. E15, 18-2012-15 (Dubna, 2012), p. 65.
20. J. Sethi, R. Palit, S. Saha, et al., Phys. Lett. B **725**, 85 (2013).
21. J. J. Carroll, M. S. Litz, K. A. Netherton, et al., AIP Conf. Proc. **1525**, 586 (2013).
22. S. S. Dietrich and B. L. Berman, At. Data Nucl. Data Tables **38**, 199 (1988).
23. J. Blachot, Nucl. Data Sheets **91**, 135 (2000).